The fatigue failure study of repaired aluminum plates by composite patches using Acoustic Emission

Maleki, Abdullah; Saeedifar, Milad; Ahmadi Najafabadi, Mehdi; Zarouchas, Dimitrios

DOI
10.1016/j.engfracmech.2017.12.034

Publication date
2019

Document Version
Final published version

Published in
Engineering Fracture Mechanics

Engineering Fracture Mechanics 210 (2019) 300–311

Contents lists available at ScienceDirect

Engineering Fracture Mechanics

journal homepage: www.elsevier.com/locate/engfracmech

The fatigue failure study of repaired aluminum plates by composite patches using Acoustic Emission

Abdullah Maleki [a], Milad Saeedifar [a,b], Mehdi Ahmadi Najafabadi [a,*], Dimitrios Zarouchas [b]

[a] Non-destructive Testing Lab, Department of Mechanical Engineering, Amirkabir University of Technology, 424 Hafez Ave, 15914 Tehran, Iran
[b] Structural Integrity & Composites Group, Faculty of Aerospace Engineering, Delft University of Technology, The Netherlands

ARTICLE INFO

Article history:
Received 14 November 2017
Received in revised form 18 December 2017
Accepted 22 December 2017
Available online 24 December 2017

Keywords:
Repaired cracked-aluminum
Composite patch
Acoustic Emission
Fatigue
Fractography

ABSTRACT

The aim of this study is to investigate the failure of cracked aluminum plates repaired by one-side composite patches under fatigue loading using Acoustic Emission (AE) and fractography images. Rectangular specimens made of 6061 aluminum alloy with central through thickness pre-cracks were repaired using glass/epoxy laminated patches. The specimens were subjected to the fatigue loading and AE technique was employed to monitor the effect of the repair patch on the damage progression. First, different stages of damage evolution were studied based on the mechanical data and fractography images. Then, the AE energy utilized to characterize failure process of the specimens. To this aim, AE signals of the aluminum cracking and adhesive layer failure were discriminated according to their energy content. The effect of patch thickness and layup on the failure behavior of the specimens were also studied. Finally, it is concluded that AE is a powerful technique to characterize the failure process of a repaired cracked aeronautic structure by composite patches.

1. Introduction

The aluminum alloys are widely used in the aeronautic and maritime fields due to their advantages such as low density, high strength, and good corrosion resistance [1]. However, they are susceptible to cracking in severe operational conditions [2]. Extending the service life of cracked parts in the aerospace industry is an interesting subject that attracted many researchers to investigate it during the last decades [3–12]. There are different methods to repair the aeronautic cracked aluminum parts such as: filling the cracked region with a proper filler alloy by a suitable welding procedure [13], or drilling of the crack tip with a small diameter drill bit and then attaching a metal skin to that region by rivets [14–16]. However, each of these methods has some disadvantages. For example, welding could introduce hot cracking susceptibility to the aluminum and rivets could introduce some stress concentration around the crack region [17]. An alternative and very promising method is using adhesively-bonded composite patches that is widely utilized for repairing of cracked aeronautic structures [7–12,18,19]. Some advantages of repairing the cracked structures by the composite patches are high stiffness, high fatigue life, low weight, and low cost and time of repairing process [20]. One of the most common failure mechanisms of the repaired cracked structures by the adhesively-bonded composite patches is patch debonding caused by residual stresses due to thermal mismatching of the patch and structure or existing of some impurities at the interface before patch attaching [12,21,22].

* Corresponding author.
E-mail address: ahmadin@aut.ac.ir (M. Ahmadi Najafabadi).

https://doi.org/10.1016/j.engfracmech.2017.12.034
0013-7944/

There are many studies about the investigation of the repaired cracked structures with composite patches. Some studies investigated the lifetime of patched structures and its effective parameters such as patch material, layup and surface preparation using numerical, analytical and experimental approaches [23–28]. Hosseini Toudeshky et al. [27,28] conducted numerical and experimental studies on the effect of patch layup on the fatigue crack propagation of a repaired cracked aluminum plate and reported that the life of the repaired specimen may be increased by the order of 30–85% depending on the patch layup. Errouane et al. [2] studied the failure of patched repaired aluminum by a numerical model to optimize the patch design. They reported that because of shear lag effects, short patches with insufficient height are not recommended.

Acoustic Emission (AE) is a rapidly growing technique for damage detection and Structural Health Monitoring (SHM) of metal and composite materials [29–31]. Many researchers utilized AE to characterize the behavior of interlaminar and intralaminar damages such as matrix cracking, fiber breakage, and layers debonding in laminated composites [32–38]. However, according to the literature review, it was found that there are only a few studies on the investigation of the failure of the repaired cracked structures by composite patches using AE technique. Gu et al. [22] monitored the quasi-static fracture of a cracked aluminum repaired by a composite patch using the AE. They classified damage mechanisms by their frequency ranges. However, some significant overlaps were observed between the frequency ranges of the different damages. Okafor and Singh [39,40] predicted the fatigue crack growth in a composite patch repaired cracked aluminum using Neural Network (NN) and AE. They used the AE event number for training the NN to predict fatigue crack growth. None of these studies investigated the failure process of the repaired specimens by the fractography images. Thus, in this paper a comprehensive study has been conducted on the investigation of the failure process of the composite patch repaired cracked aluminum using the fractography and AE data. Also, due to the complete overlap of the frequency range of the damage mechanisms, a new AE parameter is used to damage clustering instead of the frequency parameter.

This paper focuses on the study of the failure process of a cracked aluminum repaired by a composite patch under fatigue loading using AE technique and fractography images. The rectangular specimens made of 6061 aluminum alloy with central through thickness pre-cracks were repaired by glass/epoxy laminated patches. The behavior of damage evolution during fatigue loading was comprehensively investigated by the fractography images and AE parameters. Also, the AE signals of the aluminum cracking and adhesive layer failure were differentiated according to their energy. In addition, the effects of the patch thickness and layup on the failure behavior of the specimens were investigated. The results showed that AE could predict the failure of the adhesive layer and also could detect and distinguish different damage mechanisms. Thus, it is concluded that AE is a powerful technique for structural health monitoring of the patch repaired aeronautic structures under fatigue loading conditions.

2. Experimental procedures

2.1. Description of the materials

The rectangular specimens were fabricated of 6061 aluminum alloy with a central through-thickness pre-crack. In order to insert the pre-crack, first, a notch with 0.4 mm in width and 9.1 mm in length was formed in the center of the specimens by wire-cut machining. Then, the specimens were subjected to the fatigue loading to introduce pre-cracks, so as the total length of notch and fatigue pre-crack was 13 mm. The fatigue pre-crack length was measured using a digital camera with the 220X zoom and image processing technique. Due to this fact that the pixels of the crack are darker than the surrounding pixels, the image processing algorithm uses the color difference between the pixels of the crack with the surrounding pixels to track the crack path. It starts with the first pixel of the crack, then it reduces the darkness of this pixel, then it gets the second dark pixel around the first one. This loop is repeated until the final point of the crack is detected. Then, the number of pixels is converted to millimeter. The fatigue loading parameters for introducing the fatigue pre-crack in the specimens are 30 kN, 3 kN, and 10 Hz, for maximum load, minimum load, and load frequency, respectively, which were extracted from the S-N curve of aluminum. The cracked aluminum specimen is illustrated in Fig. 1a. The surface of the specimens was washed, etched, and chromatid to be prepared for attaching the composite patches. The composite patches were fabricated from prepregs of unidirectional glass/epoxy composites (®GURIT). The patches were attached to the aluminum specimens by the epoxy-based glue XB5047/XB5067 (®Huntsman). A view of the repaired specimens is shown in Fig. 1b. In order to study the effect of patch layup and patch thickness on the fatigue lifetime of the repaired specimens, 5 groups of the specimens were fabricated. The specification of the specimens is represented in Table 1.

2.2. Test method

The specimens were subjected to the tensile cyclic loading until the final fracture (see Fig. 2). The tests were performed under load control mode and the loading parameters were as follows: the maximum load was 25 kN, the minimum load was 2.5 kN, and the load frequency was 10 Hz. A calibrated universal tensile/compression machine (DARTEC) was used to load the specimens at a temperature of 25 °C. The load cell capacity of the machine was 50 kN with ±100 N resolution. The applied load and vertical displacement were recorded during all the tests by the machine. The crack growth in aluminum was also continuously recorded during the tests by a microscope digital camera with 220X zoom which was positioned at the behind

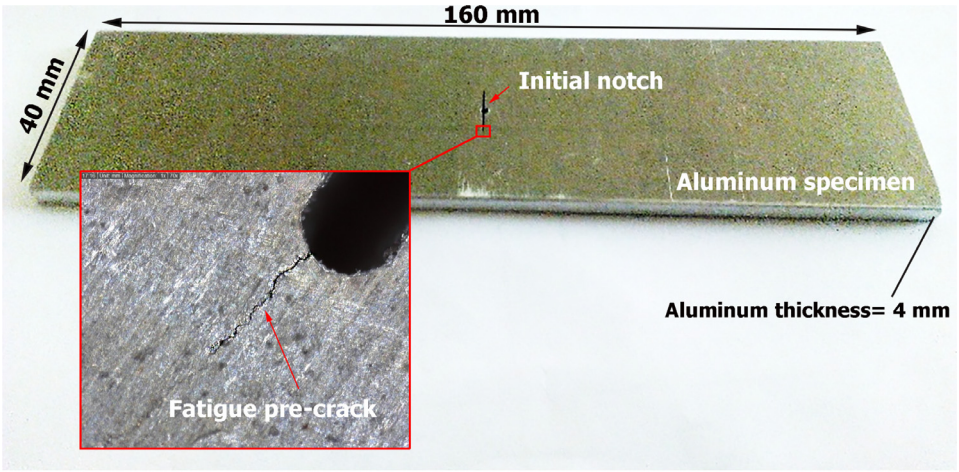

(a)

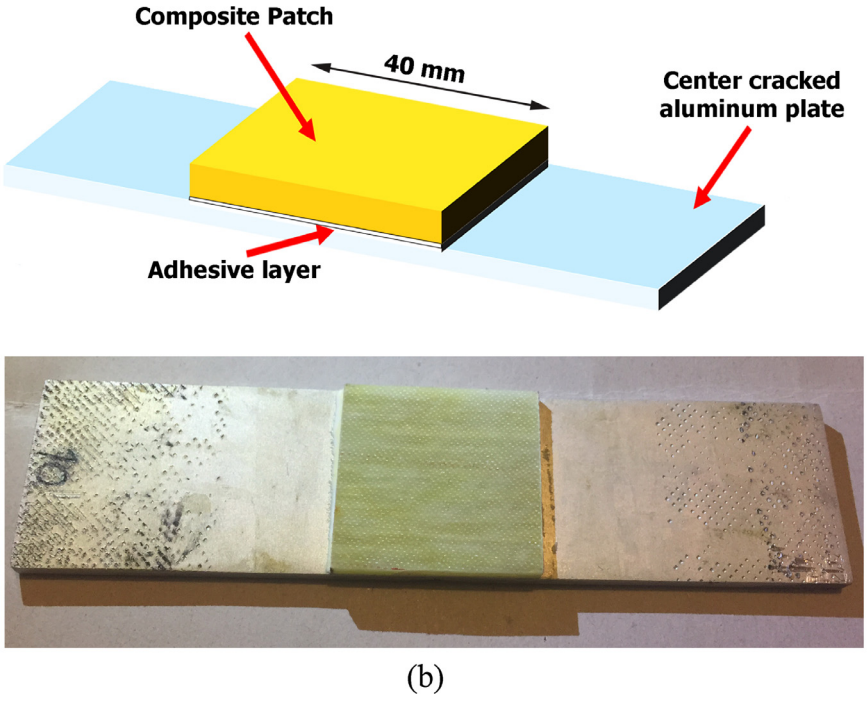

(b)

Fig. 1. (a) The cracked aluminum specimens, and (b) the repaired specimens.

Table 1
The specification of the specimens.

Specimens	Number of layers	Lay-ups
S_{Al}	–	–
S_{4C}	4	$[0^\circ/90^\circ]_S$
S_{4U}	4	$[0^\circ_4]$
S_{8U}	8	$[0^\circ_8]$
S_{16U}	16	$[0^\circ_{16}]$

Subscripts of Al, C, and U are referred to Aluminum, Cross-ply, and Unidirectional, respectively.

of the specimens. Two AE sensors, which were placed on the Al specimen surface recorded the originated AE signals. Four coupons of each specimen type were tested to check the tests reproducibility.

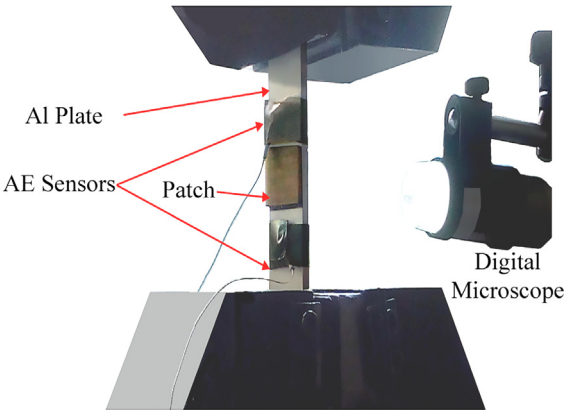

Fig. 2. The test setup.

2.3. AE sensors

In order to record the AE events of the specimens, two AE sensors were mounted on the specimen surface. The utilized AE sensors, PICO, were the single-crystal piezoelectric transducer, broadband, and resonant-type from Physical Acoustics Corporation (PAC). The resonance frequency and optimum operating frequency range of the AE sensors were 513.28 kHz and [100–750 kHz], respectively. AE events were recorded by using the acoustic emission software, AEWin, and a data acquisition system PAC-PCI-2 with a maximum sampling rate of 40 MHz. A vacuumed silicon grease was used as the acoustical coupling. The recorded AE signals by the AE sensors were enhanced by the 2/4/6-AST preamplifiers. The gain selector of the preamplifiers was set to 37 dB. The test-sampling rate was 1 MHz with 16 bits of resolution between 10 and 100 dB. The threshold of receiving AE signals was adjusted to 35 dB.

3. Results and discussions

3.1. Mechanical and fractography results

Fig. 3 shows the vertical displacement and Crack Tip Opening Displacement (CTOD) versus the cycles number curves for the unrepaired (S_{Al}) and the repaired (S_{8U}) specimens. The values of CTOD were calculated by counting the number of pixels at the crack tip using the image processing technique during the fatigue test. The displacement curve of the unrepaired specimen can be divided into three regions. In the first region (R.1), the vertical displacement increases with an infinitesimal rate until 8600 cycles. This region corresponds to the brittle fatigue crack growth. At cycles number 8600, the length of the crack has been increased considerably, thus, the effective stress at the crack tip is high. Therefore, size of the plastic zone at the crack tip gets larger and consequently the behavior of crack propagation switches from the brittle fracture to the ductile tearing. Thus, in the second region (R.2), the displacement increases rapidly. At the third region (R.3), the ligament length has been very small, thus, the aluminum specimen is completely fractured suddenly at the cycles number 10,915. The CTOD curve also consists with the displacement curve. Accordingly, the CTOD increases with a small rate in the first region. While, increasing rate of CTOD significantly rises at the beginning of the second region. At the final region, the CTOD increases sharply.

The displacement curve of the repaired specimen (S_{8U}) can be divided into three regions as similar to the unrepaired specimen. At the first region which the patch is firmly attached to the aluminum, the vertical displacement increases with a low rate. The rate of vertical displacement in this region for the repaired specimen is 15% less than the rate of vertical displacement for the unrepaired specimen which is due to the effect of patch. This region is extended to 26,000 cycles. In this region, the CTOD increases with an infinitesimal rate. This is due to the fact that the patch is still attached to Al, thus a major portion of the applied load has been carried by the patch and the effective applied load on Al is small. At cycles number 26,000, there is a big jump in the displacement curve which corresponds to the failure of the adhesive layer and local separation of the composite patch from the aluminum plate. The experimental observations also detect this phenomenon. After adhesive layer failure, the effective applied load on Al increases and consequently the vertical displacement and CTOD increase faster. The increasing rate of displacement is almost constant up to 32,000 cycles. The rate of vertical displacement in the second region for the repaired specimen is 58% less than the rate of vertical displacement for the unrepaired specimen. At this cycle number, the behavior of fracture changes from the brittle fatigue crack growth to the ductile tearing. Thus, at the third region, vertical displacement and CTOD increase precipitately and consequently the final fracture of the aluminum specimen occurs at cycles number 33,000.

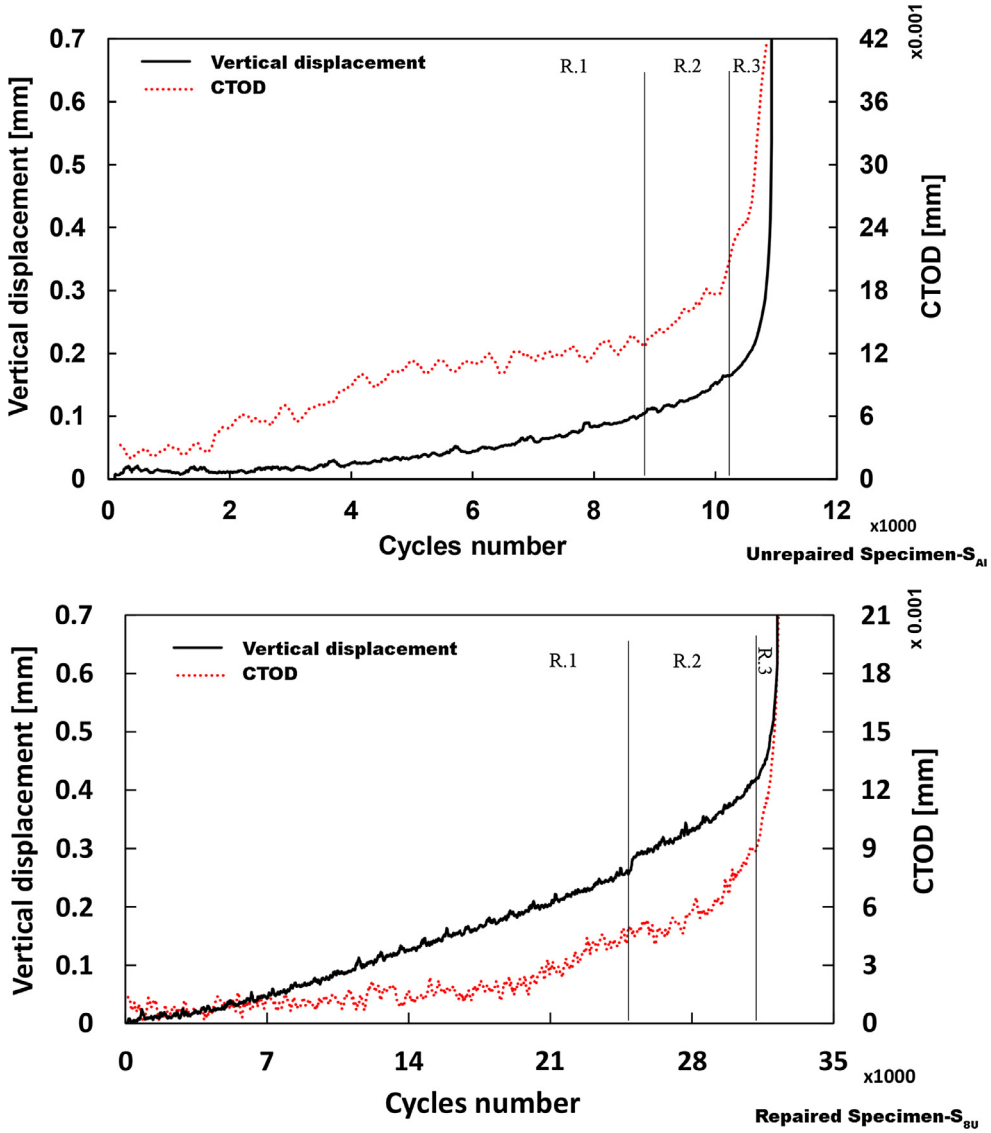

Fig. 3. The vertical displacement and CTOD versus the cycles number for the unrepaired and the repaired specimens.

Fig. 4 shows the fractured surface of the unrepaired and repaired specimens. As can be seen, the length of brittle fatigue crack growth region for the repaired specimen is bigger than this region for the unrepaired specimen. This fact shows that the composite patch could significantly increase the fatigue life of the cracked aluminum. Comparison of the cycles number to the final failure of the unrepaired and repaired specimens also confirms this claim (see Fig. 3). In the case of the repaired specimen, it is obvious that the length of fatigue crack growth at the repaired side is smaller than from the unrepaired side. Due to the attaching of the composite patch to the repaired side, the effective applied stress to the crack edge at this side is smaller than from the unrepaired side. Thus, due to the higher applied stress at the unrepaired side, the crack would like to deviate to the unrepaired side. Fig. 5 shows the value of the effective applied stress at the two sides of the repaired specimen which has been obtained from the theoretical calculations [41]. S_1 shows the stress component along the loading direction and S_2 illustrates the stress component perpendicular to the loading direction. To calculate the applied stress, the repaired specimen was considered as a 6 layers laminated composite consisting of 4 layers of unidirectional glass/epoxy, one layer of the adhesive, and one layer of the aluminum. Then, the stresses in each layer were calculated based on the theoretical fundamentals for calculation of the stress in laminated composites under longitudinal tension loading condition [41]. As can be seen, for the repaired specimen (S_{4U}) the value of longitudinal S_1 stress at the repaired and unrepaired sides is 80 MPa and 210 MPa, respectively. Thus, crack likes deviate from the straight line to the unrepaired side. The patterns of fatigue crack growth in the SEM images of the fractured surface of the specimens confirm this claim (see Fig. 4). Accordingly, the brittle fatigue crack growth for the unrepaired specimen is along the orientation of fatigue pre-crack while for the repaired specimen the fatigue crack growth deviates to the unrepaired side.

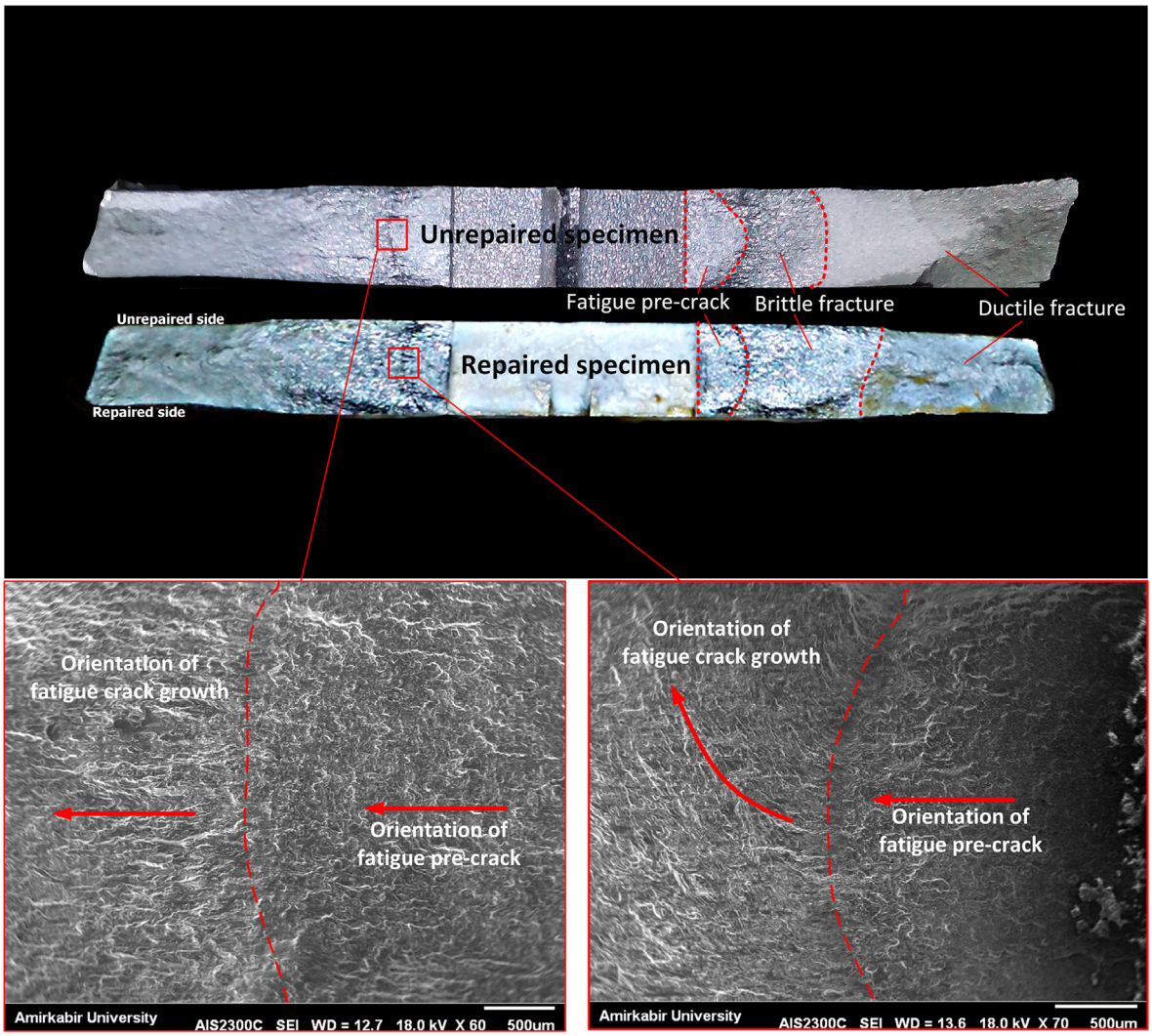

Fig. 4. The fracture surface of the unrepaired and repaired specimens.

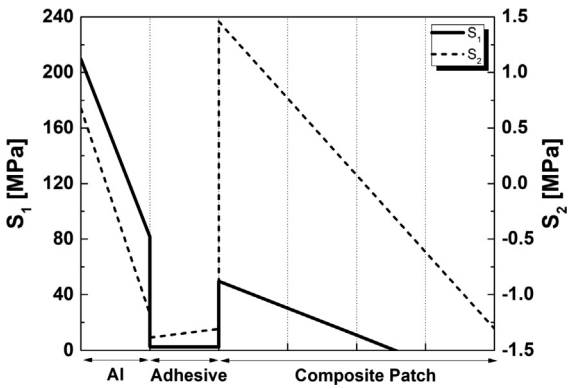

Fig. 5. The effective applied stress at the two sides of the repaired specimen.

Fig. 6 shows the SEM images of the fractured surface of the unrepaired and repaired specimens. The dominant fracture mechanism in the brittle fatigue crack growth zone is cleavage. Also, the fractured surface in this region is perpendicular

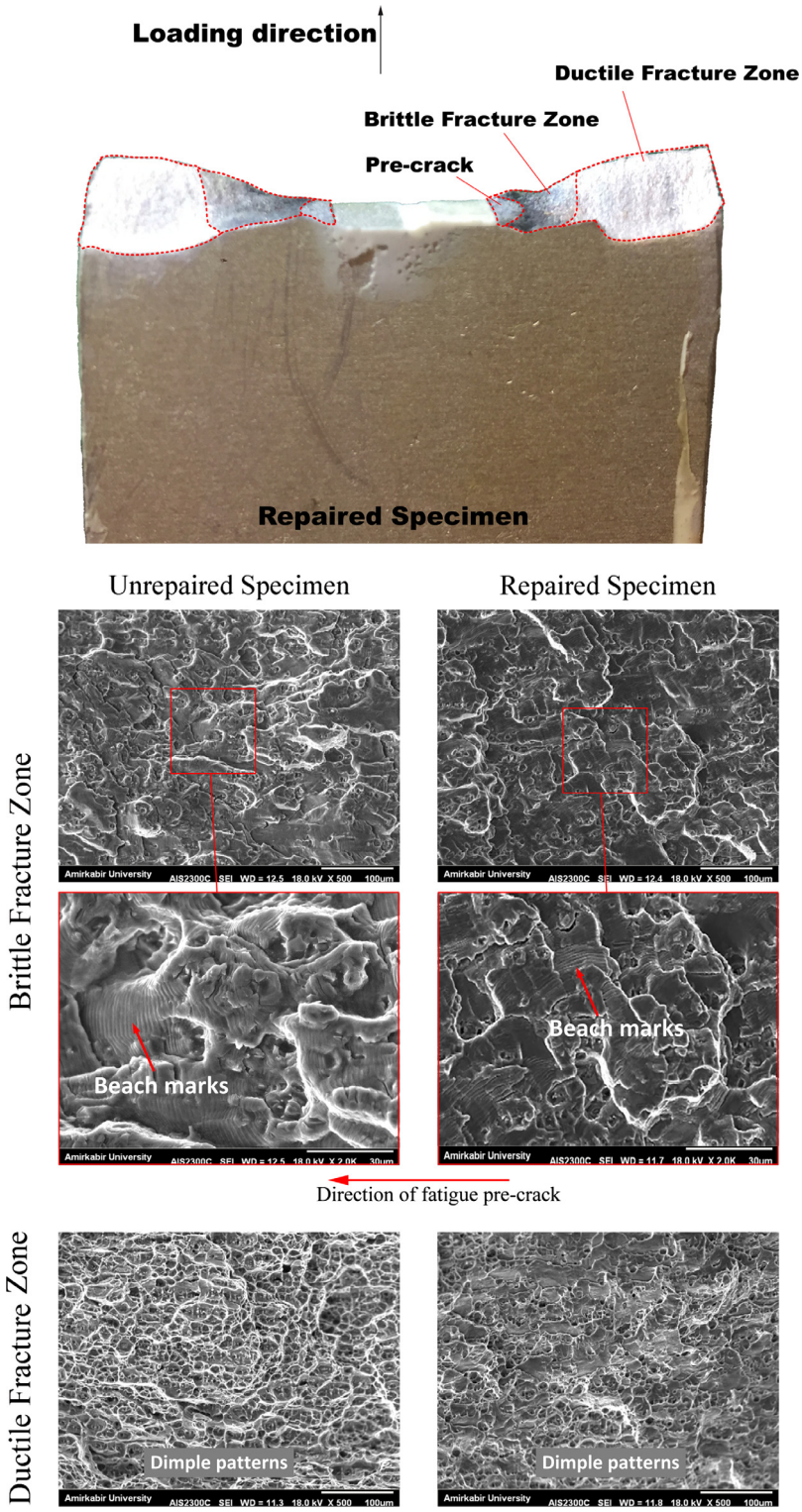

Fig. 6. The SEM images from the fractured surface of the unrepaired and repaired specimens.

to the applied load direction. These two facts confirm the brittle behavior of the fatigue crack growth in this region, while micro voids and their coalescence are the dominant fracture mechanisms in the ductile fracture zone which corresponds to the ductile tearing. Also, the angle of the fractured surface in this region with the applied load direction is about 45° which is

consistent with the theory of ductile fracture [42,43]. The beach marks of fatigue crack growth show that the crack growth of the unrepaired specimen is parallel to the pre-crack direction while the crack growth of the repaired specimen deviated to the unrepaired side.

3.2. AE results

Fig. 7 shows the cumulative AE energy and vertical displacement versus the cycles number for the unrepaired and repaired specimens. The cumulative AE energy for the unrepaired specimen increases with an infinitesimal rate in the brittle fatigue crack growth region, while, in the ductile tearing region, it increases rapidly. At cycles number 10,915 which the specimen is fractured suddenly, the cumulative AE energy rises by a big jump.

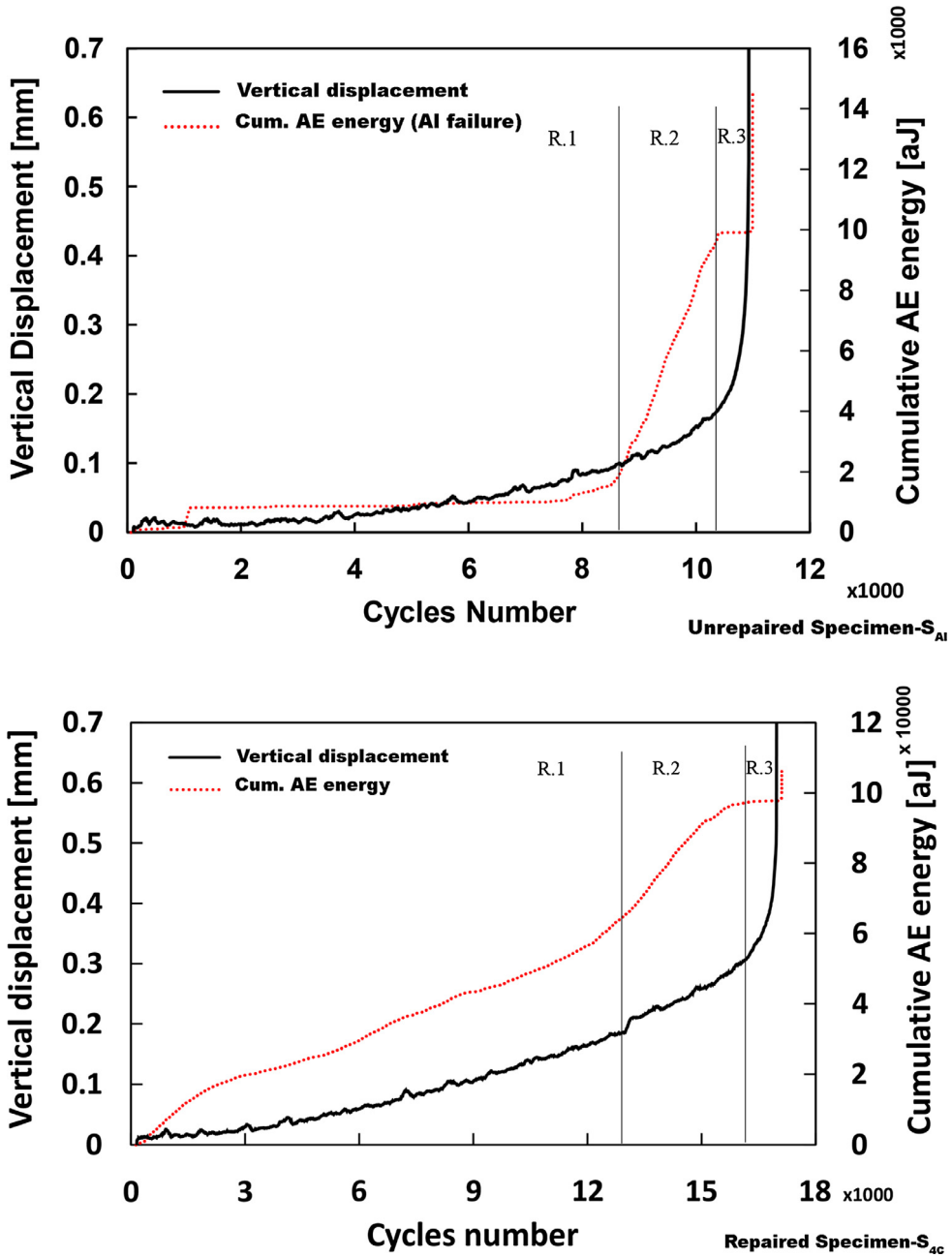

Fig. 7. The cumulative AE energy and vertical displacement versus the cycles number for the unrepaired and repaired specimens.

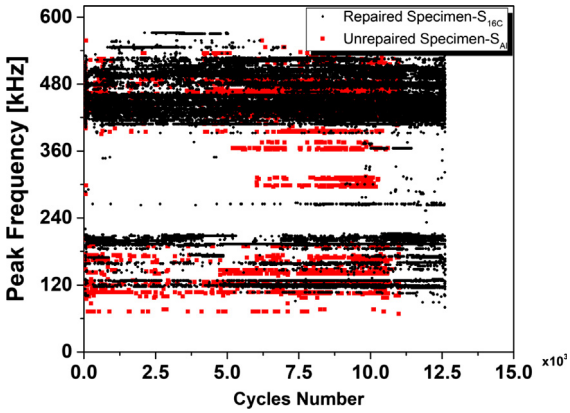

Fig. 8. The frequency distribution of AE signals for the unrepaired and repaired specimens.

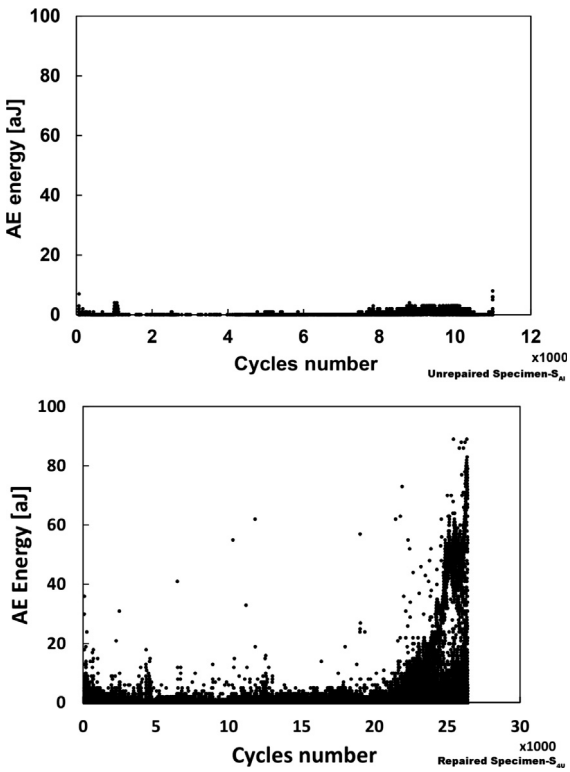

Fig. 9. The AE energy versus cycles number for the unrepaired and repaired specimens.

The cumulative AE energy curve of the repaired specimen is divided into three regions as same the regions of Fig. 3. In the first region which the patch is firmly attached to the aluminum, the slope of the cumulative AE energy curve is low. In this region, composite patch carries a considerable portion of the applied load, thus the rate of crack growth in aluminum and consequently the AE activities of the specimen are low. At the point of the adhesive layer failure (cycles number 12,800), the vertical displacement rises by a significant jump and the slope of cumulative AE energy curve increases. The increase of cumulative AE energy is due to the generating of adhesive layer failure signals. In the second region, the cumulative AE energy increases with a higher rate in comparing with the first region. In this region, due to the failure of the adhesive layer, the applied load is completely carried by Al. Therefore, the crack growth rate and consequently AE activities of the specimen increase. In the ductile tearing region, which the damage evolution has accelerated, the cumulative AE energy increases with the maximum rate. Due to the mixing of AE signals of Al cracking and adhesive layer failure, it is not possible to individually investigate the state of each damage mechanism during the test. In order to detect the failure of adhesive layer and separation of the patch with more accurate, it is needed to distinguish the AE signals of adhesive layer failure from the Al failure.

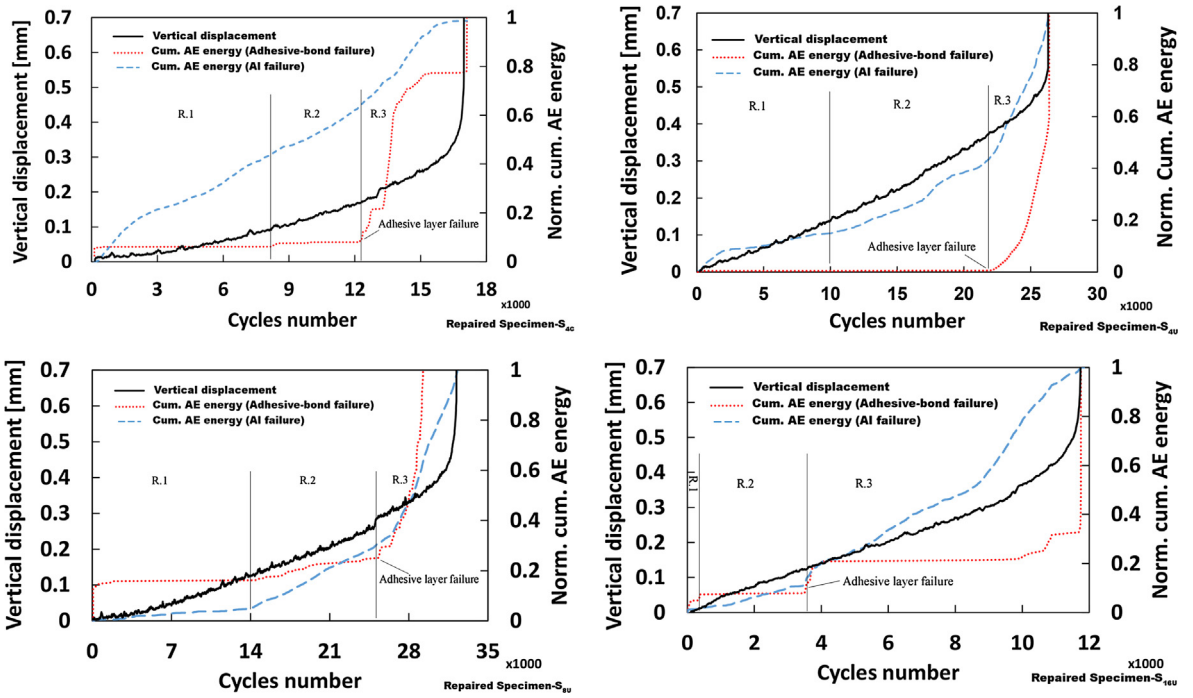

Fig. 10. The normalized cumulative AE energy versus cycles number curves of the Al cracking and adhesive layer failure for the repaired specimens.

In the previous study on the AE-based failure analysis of patch repaired cracked aluminum under static loading [22], the frequency was utilized for discrimination of the Al cracking signals from the adhesive layer failure signals. However, as being reported in that research, there is a significant overlap between the frequency range of the Al cracking and the adhesive layer failure. Fig. 8 shows the frequency distribution of the AE signals for the unrepaired and repaired specimens. As can be seen, in the frequency distribution of the unrepaired specimen there are two groups of signals with frequency band [80–200 kHz] and [350–600 kHz] that they are dedicated to aluminum cracking, the only damage mechanism. On the other hand, based on the experimental observations during the tests, besides the Al cracking, there is another damage mechanism in the repaired specimens, i.e. adhesive layer failure. It should be mentioned that due to high stiffness of all patches there was not any composite patch fracture during all the tests and only adhesive layer failure and separation of patches were observed. The frequency distribution of the repaired specimen is completely similar to the unrepaired specimen and there is not any new private frequency range for the adhesive layer failure and its frequency has a complete overlap with the Al cracking signals. Thus, the frequency parameter cannot be used for damage clustering in this case. By investigation of different AE parameters, it was found that the energy of the AE signals is a good parameter for the Al and adhesive layer failures clustering. Fig. 9 shows AE energy versus cycles number for the unrepaired and repaired specimens. As can be seen, the energy of all AE signals of the unrepaired specimen is less than 8 aJ, while in the case of the repaired specimen, besides the signals with the energy below 8 aJ, there are some other signals with the energy higher than 8 aJ. Accordingly, the AE signals with the energy below 8 aJ are dedicated to Al cracking and the AE signals with the energy higher than 8 aJ are devoted to the adhesive layer failure.

The AE signals of the repaired specimens were classified according to their AE energy. The normalized cumulative AE energy versus cycles number curves of the Al cracking and adhesive layer failure for the repaired specimens are shown in Fig. 10. A big jump in the cumulative AE energy curve of adhesive layer failure at the initiation of tests is related to fracture of the little adhesive material which has penetrated to the notch of the aluminum specimen. Besides this jump, all the figures can be divided into three regions. In the first section, almost there are no AE signals of adhesive layer failure. While the AE signals of Al cracking initiate from the beginning of the tests and increase with a low rate. At the end of this region, the adhesive layer failure signals initiate. These signals are referred to some micro damages in the adhesive layer. After some cycles, the energy curve of adhesive layer failure starts to increase with a very high rate. This point corresponds to the significant adhesive layer failure and separation of the patch from the aluminum specimen. In the second region, due to the failure of the adhesive layer, the applied load on the Al specimen increases, and consequently the regime of fracture changes from the brittle fracture to the ductile tearing, therefore the AE signals of Al cracking increases with a higher slope. Thus, the first big jump in the cumulative AE energy curve of adhesive layer failure signals is considered as the point of adhesive layer failure.

Fig. 11 represents the cycles number to the final failure of the specimens and also the cycles number to the failure of the adhesive layer which is detected by the cumulative AE energy curve of adhesive layer failure. It is obvious that at a fixed

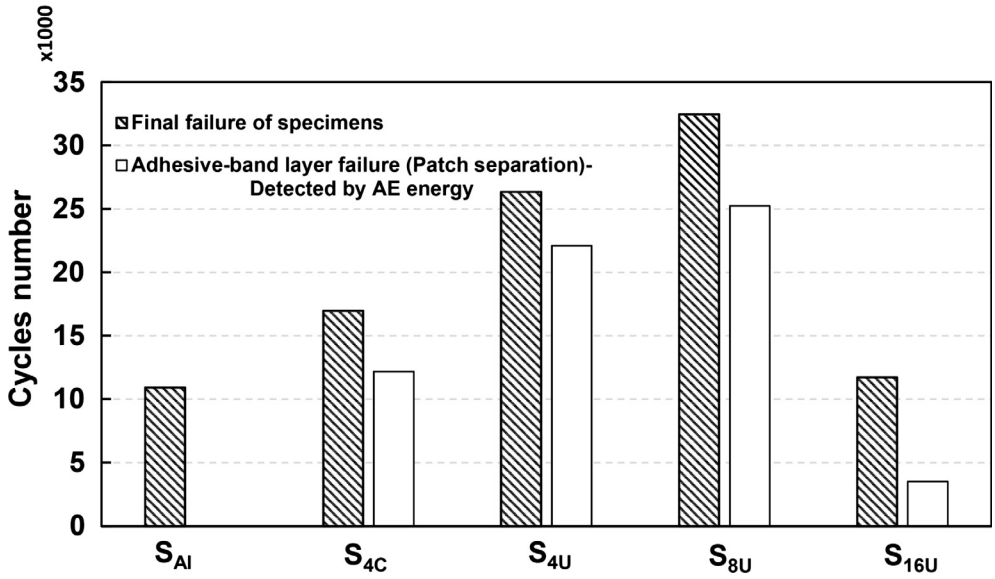

Fig. 11. The cycles number to the final failure of the specimens and the cycles number to the failure of adhesive layer obtained from AE.

patch thickness (4 layers), the unidirectional layup (S_{4U}) has the better performance in comparison with the cross-ply layup (S_{4C}) and it could improve the lifetime of the cracked aluminum with 141% against 55% for the cross-ply layup. However, the remained lifetime after separation of the patch for the S_{4C} is higher than S_{4U} (4790 cycles for S_{4C} against 4223 cycles for S_{4U}). Due to the higher stiffness of the unidirectional patch, it carries more portion of the applied load, thus when it is failed more additional load is applied to the Al specimen. On the other hand, at a fixed layup, the best thickness for the patch is for the 8 layers patch that could improve the fatigue life about 197%. The better functionality of specimen S_{8U} is due to this fact that this specimen has a big stiffness and it does not also induce a big bending moment to the specimen. In contrary, the specimen S_{16U} has the worst functionality. Although the 16 layers patch has a bigger stiffness, but, because of the high thickness of the patch, it induces a big bending moment to the specimen that leads to the separation of the patch from Al at the low cycles number.

4. Conclusions

In this study, an experimental investigation was conducted on the characterization of fatigue fracture of cracked aluminum repaired with composite patches using the fractography images and AE technique. To this aim, the center through-thickness cracked aluminum specimens were repaired by glass/epoxy composite patches with different layups and thicknesses. The behavior of the damage evolution during the fatigue loading was comprehensively investigated by the fractography images and the AE energy parameter. Also to accurately detect the failure of the adhesive layer, the AE signals of the aluminum cracking and adhesive layer failure were discriminated. It was found that the frequency parameters that implemented by some previous researchers to damage clustering is not an informative parameter to damage classification in this case due to the overlap of the frequency range of the Al cracking and the adhesive layer failure. Therefore, the energy of the AE signals was selected for the data clustering. It was found that the Al cracking generates AE signals with the energy less than 8 aJ while adhesive layer failure generates the AE signals with the energy higher than 8 aJ. Accordingly, the point of patch separation from the repaired specimens is detected using the AE signals of adhesive layer failure. In addition, the effect of patch thickness and layup on the fatigue life of the repaired specimens were studied. It was found that the best functionality is for the 8 layers patch that improved the fatigue life of the cracked aluminum about 197% while the worst functionality is for the 16 layers patch that only improved the fatigue lifetime about 7%. The results showed that AE could be utilized for different damages detection and classification and it is a powerful method for structural health monitoring of the patch repaired aeronautic structures subjected to fatigue loading.

References

[1] Wen Y, Meng H, Shang W. Corrosion resistance and adsorption behavior of bis-(γ-triethoxysilylpropyl)-tetrasulfide self-assembled membrane on 6061 aluminum alloy. RSC Adv 2015;5:80129–35.
[2] Errouane H, Sereir Z, Chateauneuf A. Numerical model for optimal design of composite patch repair of cracked aluminum plates under tension. Int J Adhes Adhes 2014;49:64–72.
[3] Baker AA, Callinan RJ, Davis MJ, Jones R, Williams JG. Repair of mirage III aircraft using the BFRP crack-patching technique. Theor Appl Fract Mech 1989;2(1):1–15.

[4] Buxbaum O, Huth H. Expansion of cracked fastener holes as a measure for extension of lifetime to repair. Eng Fract Mech 1987;28(5–6):689–98.
[5] Baker AA, Rose LRF, Jones R. Advances in the bonded composite repair of metallic aircraft structure. Elsevier Science; 2003.
[6] Pramanik A, Basak AK, Dong Y, Sarker PK, Uddin MS, Littlefair G, et al. Joining of carbon fibre reinforced polymer (CFRP) composites and aluminium alloys – a review. Compos A 2017;101:1–29.
[7] Park SY, Choi WJ, Choi HS. A review of the recent developments in surface treatment techniques for bonded repair of aluminum airframe structures. Int J Adhes Adhes 2017. doi: https://doi.org/10.1016/j.ijadhadh.2017.09.010.
[8] Sabelkin V, Mall S, Hansen MA, Vandawaker RM, Derriso M. Investigation into cracked aluminum plate repaired with bonded composite patch. Compos Struct 2007;79(1):55–66.
[9] Wen SW, Xiao JY, Wang YR. Accelerated ageing behaviors of aluminum plate with composite patches under salt fog effect. Compos B 2013;44(1):266–73.
[10] Pavlopoulou S, Grammatikos SA, Kordatos EZ, Worden K, Paipetis AS, Matikas TE, et al. Continuous debonding monitoring of a patch repaired helicopter stabilizer: damage assessment and analysis. Compos Struct 2015;127(1):231–44.
[11] Schubbe JJ, Bolstad SH, Reyes S. Fatigue crack growth behavior of aerospace and ship-grade aluminum repaired with composite patches in a corrosive environment. Compos Struct 2016;144:44–56.
[12] Zarrinzadeh H, Kabir MZ, Deylami A. Crack growth and debonding analysis of an aluminum pipe repaired by composite patch under fatigue loading. Thin Walled Struct 2017;112:140–8.
[13] Shankar K, Wu W. Effect of welding and weld repair on crack propagation behaviour in aluminium alloy 5083 plates. Mater Des 2002;23(2):201–8.
[14] Newman JC, Ramakrishnan R. Fatigue and crack-growth analyses of riveted lap-joints in a retired aircraft. Int J Fatigue 2016;82(part 2):342–9.
[15] Huang L, Guo H, Shi Y, Huang S, Su X. Fatigue behavior and modeling of self-piercing riveted joints in aluminum alloy 6111. Int J Fatigue 2017;100(part 1):274–84.
[16] Huang L, Shi Y, Guo H, Su X. Fatigue behavior and life prediction of self-piercing riveted joint. Int J Fatigue 2016;88:96–110.
[17] Maligno AR, Soutis C, Silberschmidt VV. An advanced numerical tool to study fatigue crack propagation in aluminium plates repaired with a composite patch. Eng Fract Mech 2013;99:62–78.
[18] Baker AA, Chester RJ. Recent advances in bonded composite repair technology for metallic aircraft components. In: Proceeding of the international conference on advanced composite materials; 1993. p. 45–9.
[19] Nishino M, Aoki T. Nonlinear analysis and damage monitoring of a one-sided patch repair with delamination. Compos Struct 2006;73:423–31.
[20] Ouinas D. Effect of disbonding between a composite patch and a cracked aluminum plate on the stress intensity factor. J Reinf Plast Compos 2010;29(14):2227–36.
[21] Hosseini-Toudeshky H, Jasemzadeh A, Mohammadi B. Investigation of effective parameters on composite patch debonding under static and cyclic loading using cohesive elements. Finite Elem Anal Des 2013;74:67–75.
[22] Gu JU, Yoon HS, Choi NS. Acoustic emission characterization of a notched aluminum plate repaired with a fiber composite patch. Compos A 2012;43:2211–20.
[23] Lee WY, Lee JJ. Successive 3D FE analysis technique for characterization of fatigue crack growth behavior in composite-repaired aluminum plate. Compos Struct 2004;66(1–4):513–20.
[24] Wang QY, Pidaparti RM. Static characteristics and fatigue behavior of composite-repaired aluminum plates. Compos Struct 2002;56(2):151–5.
[25] Ouinas D, Hebbar A, Bouiadjra BB, Belhouari M, Serier B. Numerical analysis of the stress intensity factors for repaired cracks from a notch with bonded composite semicircular patch. Composites Part B 2009;40(8):804–10.
[26] Aakkula J, Saarela O. An experimental study on the fatigue performance of CFRP and BFRP repaired aluminium plates. Compos Struct 2014;118:589–99.
[27] Hosseini-Toudeshky H, Mohammadi B. Mixed-mode numerical and experimental fatigue crack growth analyses of thick aluminium panels repaired with composite patches. Compos Struct 2009;91:1–8.
[28] Hosseini-Toudeshky H, Ghaffari MA, Mohammadi B. Fatigue propagation of induced cracks by stiffeners in repaired panels with composite patches. Procedia Eng 2011;10:3285–90.
[29] Andreykiv O, Skalsky V, Serhiyenko O, Rudavskyy D. Acoustic emission estimation of crack formation in aluminium alloys. Eng Fract Mech 2010;77(5):759–67.
[30] Rabiei M, Modarres M. Quantitative methods for structural health management using in situ acoustic emission monitoring. Int J Fatigue 2013;49:81–9.
[31] De Rosa IM, Santulli C, Sarasini F. Acoustic emission for monitoring the mechanical behaviour of natural fibre composites: a literature review. Compos A 2009;40(9):1456–69.
[32] Yousefi J, Mohamadi R, Saeedifar M, Ahmadi M, Toudeshky H. Delamination characterization in composite laminates using acoustic emission features, micro visualization and finite element modeling. J Compos Mater 2016;50(22):3133–45.
[33] Mohammadi R, Saeedifar M, Hosseini Toudeshky H, Ahmadi Najafabadi M, Fotouhi M. Prediction of delamination growth in carbon/epoxy composites using a novel acoustic emission-based approach. J Reinf Plast Compos 2015;34(11):868–78.
[34] Saeedifar M, Fotouhi M, Ahmadi Najafabadi M, Hosseini Toudeshky H. Prediction of delamination growth in laminated composites using acoustic emission and cohesive zone modeling techniques. Compos Struct 2015;94(5):1483–94.
[35] Loutas T, Eleftheroglou N, Zarouchas D. A data-driven probabilistic framework towards the in-situ prognostics of fatigue life of composites based on acoustic emission data. Compos Struct 2017;161:522–9.
[36] Zarouchas D, Hemelrijck D. Mechanical characterization and damage assessment of thick adhesives for wind turbine blades using acoustic emission and digital image correlation techniques. J Adhes Sci Technol 2014;28(14–15):1500–16.
[37] Saeedifar S, Fotouhi M, Ahmadi Najafabadi M, Hossein Hosseini Toudeshky H, Minak G. Prediction of quasi-static delamination onset and growth in laminated composites by acoustic emission. Compos B 2016;85:113–22.
[38] Mohammadi R, Ahmadi Najafabadi M, Saeedifar M, Yousefi J, Minak G. Correlation of acoustic emission with finite element predicted damages in open-hole tensile laminated composites. Compos B 2017;108:427–35.
[39] Okafor AC, Singh N, Singh N, Oguejiofor BN. Acoustic emission detection and prediction of fatigue crack propagation in composite patch repairs using neural network. J Thermoplast Compos Mater 2017;30(1):3–29.
[40] Singh N, Okafor AC. Acoustic emission detection and prediction of fatigue crack propagation in composite patch repairs using neural networks. Review of Progress in Quantitative Nondestructive Evaluation, American Institute of Physics (AIP); 2007. p. 1–10.
[41] Jones RM. Mechanics of composite materials. 2ed ed. Taylor & Francis Inc.; 1999. p. 191–222.
[42] Sokolov MA, Landes JD, Lucas GE, Small specimen test techniques. 4th volume. USA: ASTM International; 2002. p. 215–7.
[43] Desquines J, Cazalis B, Bernaudat C, Poussard C, Averty X, Yvon P. Mechanical properties of zircaloy-4 PWR fuel cladding with burnup 54–64 MWd/kgU and implications for RIA behavior. J ASTM Int 2005;2(6):851–72.